Codonopis bulleynana Forest ex Diels inhibits autophagy and induces apoptosis of colon cancer cells by activating the NF-κB signaling pathway

YUNPENG LUAN[1], YANMEI LI[1], LINA ZHU[1], SHUANGQING ZHENG[2], DECHANG MAO[1], ZHUXUE CHEN[1] and YONG CAO[1]

[1]Department of Life Technology Teaching and Research, School of Life Science, Southwest Forestry University; [2]Kunming Pharmaceutical Corp., Kunming, Yunnan 652400, P.R. China

Received March 27, 2017; Accepted November 28, 2017

DOI: 10.3892/ijmm.2017.3337

Abstract. Despite its favorable clinical efficacy, oxaliplatin-based chemotherapy frequently results in treatment withdrawal and induces liver damage in colon cancer. Therefore, it is important to develop novel drugs, which can safely and effectively complement or replace the therapeutic effects of oxaliplatin. *Codonopis bulleynana* Forest ex Diels (*cb*FeD) has wide range of pharmacological effects, including anticancer effects. In the present study, the anticancer activity of *cb*FeD and its potential molecular mechanisms were investigated. *In vitro*, cell counting kit-8 assays and flow cytometry were used to assess the anti-proliferation and apoptosis-promoting activities of *cb*FeD. Transmission electron microscopy was used to monitor the autophagic vesicles. Immunofluorescence staining was performed to observe the nuclear translocation of p65 and the fluorescence of microtubule-associated protein 1 light chain 3 (LC3) B-II. The protein expression levels of p65, inhibitor of nuclear factor (NF)-κB (IκB) a, LC3B-I, LC3B-II and Beclin-1 were detected using western blot analysis. *In vivo*, the antitumor effect of *cb*FeD was assessed in colon cancer-bearing nude mice as a model. H&E staining and immunohistochemistry (IHC) were performed, with oxaliplatin set as a positive control. The results showed that *cb*FeD inhibited cell proliferation and promoted cell apoptosis in a dose-dependent manner. The effects of a high dose of *cb*FeD on colon cancer cells were similar to those of oxaliplatin. In HCT116 and SW480 cells, *cb*FeD inhibited the expression of IκBα, LC3B-I/II and Beclin-1, and the results of western blot analysis and immunofluorescence showed that, in the cells treated with *cb*FeD, p65 gradually entered nuclei in a dose-dependent manner, and the expression of LC3B-II was gradually reduced. The results of the acridine orangestaining and electron microscopy demonstrated fewer autophagic vesicles in the high-dose *cb*FeD group and the oxaliplatin group. The high dose of *cb*FeD reversed the effect of pyrrolidine dithiocarbamate, a p65-inhibitor, on the expression of p65, LC3B-I, LC3B-II and Beclin-1, and on the production of autophagic vacuoles. The high dose of *cb*FeD and oxaliplatin also suppressed tumorigenicity *in vivo*. The results of the H&E and IHC staining confirmed the inhibition of autophagy (LC3 and Beclin-1) and activation of p65 by treatment with the high dose of *cb*FeD and oxaliplatin. Taken together, *cb*FeD exhibited an antitumor effect in colon cancer cells by inhibiting autophagy through activation of the NF-κB pathway. Therefore, *cb*FeD may be a promising Chinese herbal compound for development for use in cancer therapy.

Correspondence to: Dr Yong Cao, Department of Life Technology Teaching and Research, School of Life Sciences, Southwest Forestry University, 300 Bailong Temple, Panlong, Kunming, Yunnan 652400, P.R. China
E-mail: 1820059756@qq.com

Key words: Codonopis bulleynana Forest ex Diels, oxaliplatin, autophagy, nuclear factor-κB pathway, pyrrolidine dithiocarbamate

Introduction

Colon cancer ranks as the second most common malignant tumor in Western developed countries, and is a serious threat to human life and health (1). With changes in living habits and diet, the incidence of colon cancer in China has increased substantially, and the incidence rate of colon cancer is double the global average (2-4). Therefore, the effective prevention and treatment of colon cancer has become a focus of medical investigations (3,5,6). In addition to traditional surgery, radiotherapy and chemotherapy, the combining of traditional Chinese medicine and Western medicine treatment strategies offer potential in the treatment of the colon cancer (7,8). However, the need to identify of efficient, low toxicity drugs remains. At present, natural medicine has become a focus of clinical anticancer drug investigation, due to its multi-target, multi-link and multi-channel antitumor effects.

Codonopis bulleynana Forest ex Diels (*cb*FeD) grows in the forest margin and bushes 700-200 m above sea level in the Yunnan province in China (9). It has a wide range of pharmacological effects, including its primary anticancer function. Due to the characteristics of the fresh root of *cb*FeD being unique as a national medicinal herb, few reports exist in international

journals, although there have been a wide range of investigations in China. *cb*FeD can significantly increase hemoglobin in elderly individuals with senile deficiency syndrome safety (10). Studies investigating the pharmacodynamics and acute toxicity of *cb*FeD have shown that it can enhance gastrointestinal peristalsis, improve tolerance to fatigue and hypoxia, and can promote the recovery of hemoglobin, red blood cells, IgG and the immunosuppressive effect in hemorrhagic blood-deficient mice (11,12). *cb*FeD can enhance the immune function of mice with xenograft tumors and enhance the phagocytic functions of the reticuloendothelial system (13). It has been suggested that *cb*FeD has a positive effect on chemotherapy, reducing toxicity and enhancing immune function.

Previous studies have demonstrated that signaling pathways, including autophagy, are involved in resistance to chemotherapy or radiotherapy (14,15). Autophagy, or type 2 cell death, is a regulated process, which is involved in the turnover of long-lived proteins and whole organelles, or target-specific organelles, including mitochondria and endoplasmic reticulum, to eliminate superfluity or damaged organelles (16,17). Due to the ability of autophagy to remove damaged proteins or organelles, it may paradoxically act as a mechanism for promoting the survival of irradiated cells, indicating that the inhibition of autophagy enhances radiation treatment and increases its efficacy (18). The traditional Chinese Medicine DangGuiBuXue Tang sensitizes colorectal cancer cells to chemotherapy or radiotherapy by inducing autophagy (19). Autophagy is important in cytotoxicity, infection and tumorigenesis. However, the functional role of autophagy in cancer remains controversial. Certain studies have demonstrated that autophagy inhibits the progression of tumors, whereas others have demonstrated that autophagy promotes cell death, particularly in cells resistant to apoptosis (20).

Oxaliplatin is a third-generation platinum anticancer drug, following cisplatin and carboplatin. Oxaliplatin induces autophagy and promotes the apoptosis of colon cancer cells (21-23). Oxaliplatin inhibits colorectal cancer growth and metastasis through inhibition of the nuclear factor (NF)-κB pathway (24,25). Oxaliplatin was used as control in the present study, in which the cytotoxic and antiproliferative effects of *cb*FeD on human colon cancer HCT116 and SW480 cell lines were examined. The present study also investigated the NF-κB signaling pathway modulating apoptosis and autophagy in HCT116 and SW480 cell in response to *cb*FeD treatment, and examined the consequences of inhibiting the NF-κB signaling pathway during *cb*FeD treatment using *in vivo* colon cancer models to obtain therapeutic insights.

Materials and methods

Cell culture. The HCT116 and SW480 cell lines were obtained from American Type Culture Collection (Manassas, VA, USA). The HCT116 and SW480 colon cancer cells were cultured in Dulbecco's modified Eagle's medium (DMEM) supplemented with 10% FBS (cat. no. 10099158; Gibco; Thermo Fisher Scientific, Inc., Waltham, MA, USA), 100 μg/ml of streptomycin and 100 U/ml of penicillin in a humidified atmosphere of 5% CO_2 at 37˚C.

Preparation of drug-containing serum. The dry *cb*FeD was purchased from Yunnan International Pty, Ltd. (Yunnan, China). Firstly, 1 kg of dry *cb*FeD was soaked in cold water for 30 min, decocting twice with 1:6 w/v distilled water for 1 h. Filtration was then performed to the appropriate concentrations, the first decoction comprised in 1:10 w/v distilled water for 90 min and second comprised 1:8 w/v distilled water for 60 min. A final quantity of 450 g dried powder was obtained by spray drying at room temperature, which was then sealed and stored in the dark at 4˚C. The *cb*FeD powder was dissolved in normal saline for the gavage experiments. The drug-containing serum solutions were collected from mice following exposure to the following treatments (once per day for 1 week): Treatment with normal saline by gastrogavage (n=8; normal control group); 5 g/kg of *cb*FeD by gastrogavage (n=8; low *cb*FeD group); 10 g/kg of *cb*FeD by gastrogavage (n=8; mid *cb*FeD group), 20 g/kg of *cb*FeD by gastrogavage (n=8; high *cb*FeD group); 5 mg/kg oxaliplatin by gastrogavage (n=8; oxaliplatin group). The blood samples were obtained from the abdominal aorta following treatment, following which the serum was isolated by centrifuging at 1,800 x g for 10 min at 4˚C and stored at -80˚C for the follow-up experiments.

Experimental groups. The drug-containing serum solutions from the mice were used to treat the HCT116 and SW480 cells. The five treatment groups comprised the normal control group, the low *cb*FeD group, the mid *cb*FeD group, the high *cb*FeD group, and the oxaliplatin group. For detecting the role of p65, the inhibitor pyrrolidine dithiocarbamate (PDTC) was added to a proportion of the high *cb*FeD group cells.

Cell counting kit-8 (CCK-8) assay. Cell proliferation was determined using the colorimetric water-soluble tetrazolium salt assay using a CCK-8 kit (Beyotime Institute of Biotechnology, Co., Ltd., Haimen, China). In brief, the cells at a density of $2x10^3$ cells per well was seeded in 96-well plates and incubated with the low, mid, or high dose of *cb*FeD, with or without oxaliplatin, for 24, 48 and 72 h. Following treatment, the culture medium was removed and replaced with 100 μl of fresh medium containing 10 μl of CCK-8 solution in each well and the cells were incubated at 37˚C for 2 h. The number of viable cells was determined by reading the absorbance at 450 nm using a Thermo Platemicroplate reader (Rayto Life and Analytical Science Co., Ltd., Shenzhen, China).

Cell cycle assay. Following treatment, the cells were harvested and resuspended at a density of $1x10^6$ cells/ml. The cells were fixed with ice-cold 70% ethanol for at least 30 min. Cell cycle was analyzed using a flow cytometer with propidium iodide (PI) as a specific fluorescent dye probe. The PI fluorescence intensity of 10,000 cells was measured for each sample using a Becton-Dickinson FACSCalibur flow cytometer (BD Biosciences, Franklin Lakes, NJ, USA).

Cell apoptosis assay. Following treatment, cell apoptosis was assessed using an Annexin V-FITC apoptosis detection kit (BD Pharmingen, San Diego, CA, USA). In brief, Annexin V-FITC (5 μl) and PI (5 μl) were added to 100 μl cells at a concentration of $1x10^6$ cells/ml, and incubated in the dark for 15 min at room temperature. Subsequently, binding buffer

was added and apoptosis was analyzed using flow cytometry (BD Biosciences).

Western blot analysis. The cells were harvested using protein extraction solution (Intron Biotechnology, Sungnam, Korea), and incubated for 30 min at 4˚C. Following removal of cell debris, the supernatants were collected by centrifuging at 13,000 x g for 15 min at 4˚C and the protein concentrations were determined using a Bio-Rad protein assay reagent, according to the manufacturer's protocol. Subsequently, 30 μg proteins were separated by 10% SDS-PAGE, and then transferred onto PVDF membranes. The blots were incubated with 4% bovine serum albumin (BSA; 1:200; cat. no. C0258; Beyotime Institute of Biotechnology, Co., Ltd.) blocking solution and primary antibodies against p65 (1:500; cat. no. ab16502), IκBα (1:400; cat. no. ab5076), LC3B-I/II (1:1,000; cat. no ab48394), Beclin-1 (1:500; cat. no. ab62557), GAPDH (1:1,000; cat. no. ab8245) (all from Abcam, Cambridge, MA, USA) and p-IκBα (1:400; cat. no. YK7674; Shanghai Yuanmu Biotechnology Co., Ltd., Shanghai, China) overnight at 4˚C. Following being washed three times with TBST, the blots were incubated with horseradish peroxidase-conjugated secondary antibody (1:1,000; cat. no, AB501-01A; Novoprotein Scientific, Summit, NJ, USA) for 1 h at room temperature. Following being washed three times with TBST, the blots were determined using an enhanced chemiluminescence kit (Amersham; GE Healthcare Life Sciences, Chalfont, UK).

Confocal microscopy. Immunofluorescence staining for p65 and LC3B-II was performed to precisely evaluate their expression in the cells. Following treatment, the cells were washed with ice-cold PBS and fixed in ice-cold acetone for 15 min. The cells were then blocked in 10% normal goat serum (cat. no. C0265; Beyotime Institute of Biotechnology, Co., Ltd.) at 37˚C for 1 h, following which they were washed by PBS and incubated at 37˚C with anti-p65 (1:200; cat. no. 710048) or anti-LC3B-II antibody (1:200; cat. no. 700712) (both Thermo Fisher Scientific, Inc.) for 1 h. Following three washes, the cells were incubated with FITC-conjugated goat anti-rabbit secondary antibodies (1:200; cat. no. A0562; Beyotime Institute of Biotechnology, Co., Ltd.) for 1 h at 37˚C. The slides were mounted with 4',6-diamidino-2-phenylindole (DAPI). Confocal images were captured (26) using a confocal microscope (Olympus Corp., Tokyo, Japan) at the excitation and emission wavelengths of 495 and 517 nm for FITC, 649 and 680 nm for Cy5, and 358 and 463 nm for DAPI nuclear staining, respectively.

Detection of autophagic vacuoles. The basic evidence for the induction of autophagy in cells is the formation of acidic vesicular organelles (AVOs) (27). Acridine orange was used to stain AVOs in autophagic cells. Following treatment, the cells were washed in PBS and incubated with AO (1 μg/ml) for 15 min at 25˚C (28). The cells were again washed with PBS, and AVO formation in the HCT116 and SW480 cells was observed using flow cytometry.

The presence of autophagic vesicles in HCT116 and SW480 cells was also detected using transmission electron microscopy (28). The cells were fixed in 2.5% glutaraldehyde and 2% paraformaldehyde in 0.1 M phosphate buffer (pH 7.4) for 1 h at 4˚C. Following rinsing in PBS, the cells were post-fixed in osmium tetroxide (1%) for 2 h, dehydrated in graded acetone and embedded in araldite CY212. Semi thin sections, 1 cm^2 and 1-μm-thick were cut and stained with 0.5% toluidine blue for 5 min. Ultrathin sections (50-70-nm-thick) were stained with 2% uranyl acetate and Reynold's lead citrate, and observed with a transmission electron microscope.

Xenograft tumors. A total of 18 female Balb/c athymic nude mice (5-6 weeks old, body weight 19-22 g) (Vital River Laboratories, Beijing, China) were housed at 25˚C in 40-70% humidity, in a 12 h light/dark cycle with free access to food and water and were subcutaneously injected in the right flank with $2.0x10^6$ SW480 cells in 0.1 ml PBS. When tumors had formed, the tumor volume (V) was measured using calipers daily and calculated using the following formula: $V=(LxW^2)/2$, where L was the length and W was the width of the tumor. The mice were randomly divided into three groups (n=5): Normal control group mice treated with normal saline via gavage; high dose of cbFeD (20 g/kg) mice treated with a high dose of cbFeD via gavage; oxaliplatin group mice with colon cancer treated with oxaliplatin (5 mg/kg via gavage). Growth curves were plotted using the average tumor volume within each experimental group every week. After six weeks, the mice were sacrificed, and the dissected tumors were collected and prepared for subsequent analyses. All animal experiments were approved by the Animal Center of Southwest Forestry University (Kunming, China). All experimental procedures involving animals were performed according to the institutional ethical guidelines for animal experiments and in accordance with the Guide for the Care and Use of Laboratory Animals.

IHC staining. The mice samples were fixed in 4% paraformaldehyde and endogenous enzymes were inactivated by 3% hydrogen peroxide for 10 min. Antigen retrieval was prepared by immersion in citrate buffer solution and heated at a high heat in a microwave oven for 4 min, followed by cooling and washing with PBS for 5 min. The samples were blocked in 5% BSA for 20 min at room temperature and were incubated with 50 μl primary anti body against LC3, Beclin-1 and p65 overnight at 4˚C, followed by incubation with Alexa Fluor 549 secondary antibodies (1:400; cat. no. 331594; Sigma-Aldrich; Merck KGaA, Darmstadt, Germany) for 1 h at 4˚C. Following nuclear staining, the slides were exposed to a 70, 80, 90, 100% alcohol gradient of (5 min each), and mounted with neutral gum on dry slides. Images were captured under an optical microscope.

Statistical analysis. The results are presented as the mean ± standard deviation. The statistical analysis was performed using GraphPad Prism 6 (GraphPad Software, Inc., La Jolla, CA, USA). For comparisons Dunnett t-test or two-way analysis of variance was used. $P<0.05$ was considered to indicate a statistically significant difference.

Results

Effects of cbFeD on the proliferation and cell cycle of HCT116 and SW480 cells. The *cb*FeD-containing serum solutions were prepared from mice by gastrogavage with saline (control), or 5 (low), 10 (mid) and 20 (high) g/kg of *cb*FeD. To determine

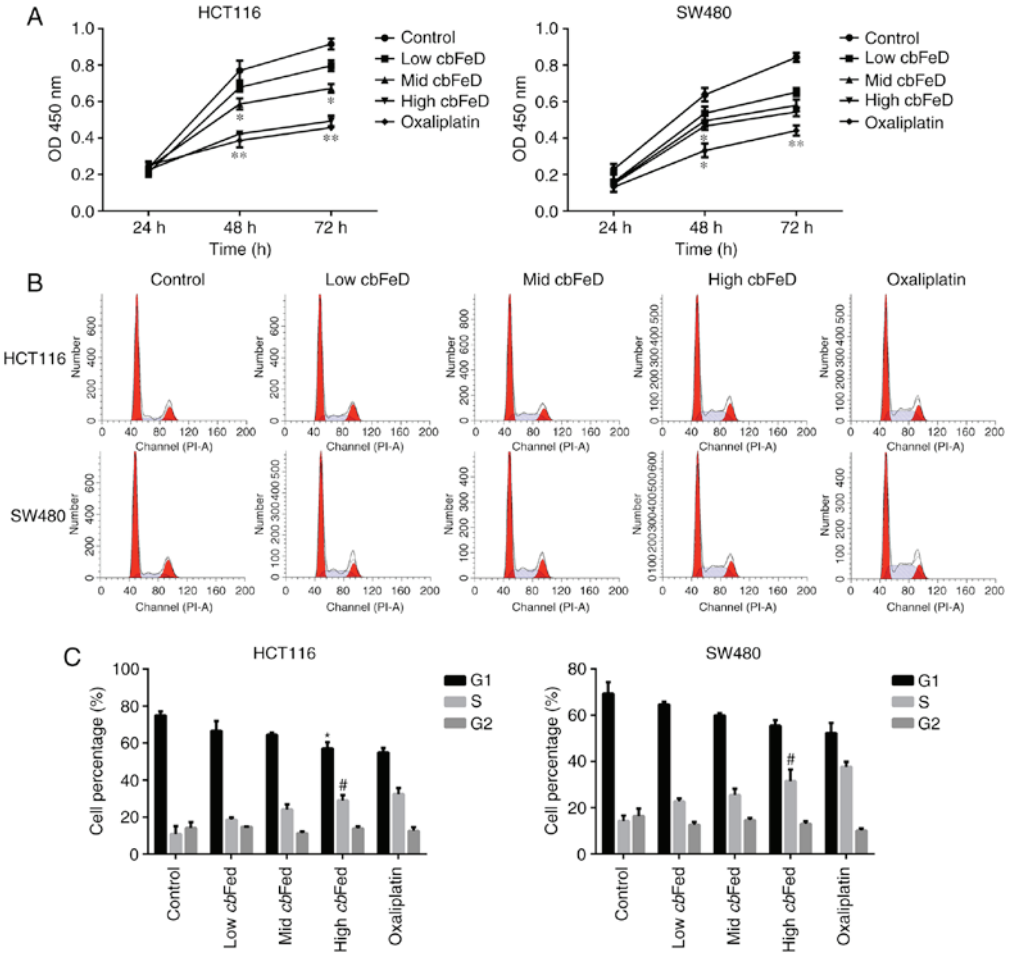

Figure 1. Effect of *cb*FeD on the proliferation and cell cycle of HCT116 and SW480 cells. Cells were treated with *cb*FeD-containing serum solutions prepared from mice treated by gastrogavage with saline (control), or 5 (low), 10 (mid) or 20 (high) g/kg of *cb*FeD for indicated durations. (A) Cell proliferation was detected using a cell counting kit-8 assay, and (B) cell cycle was detected using flow cytometry. (C) Quantification of cell cycle analysis. Oxaliplatin was used as a control. *P<0.05 vs. control; **P<0.01 vs. control; $^{\#}$P<0.05 vs. control. *cb*FeD, *Codonopis bulleynana* Forest ex Diels.

the role of *cb*FeD on cell proliferation, cell cycle and cell apoptosis, the HCT116 and SW480 cells were treated with these *cb*FeD-containing serum solutions. The results showed that *cb*FeD inhibited the proliferation of HCT116 and SW480 cells at 48 and 72 h. The cell proliferation rate was decreased with increasing concentrations of *cb*FeD-containing serum solutions, suggesting that *cb*FeD inhibited the cell proliferation in a dose-dependent manner (Fig. 1A). The cell proliferation in the high *cb*FeD group was similar to that in the oxaliplatin group. Similarly, *cb*FeD decreased the proportion of cells in the G1 phase cells, but increased the proportion of cells in the S phase, suggesting that *cb*FeD induced S phase arrest (Fig. 1B and C), which was similar to the effect of oxaliplatin. Therefore, *cb*FeD inhibited cell proliferation in a dose-dependent manner and induced cell cycle arrest at the S phase.

Effects of cbFeD on the apoptosis of HCT116 and SW480 cells. The apoptotic rates of HCT116 and SW480 cells following *cb*FeD treatment were also analyzed (Fig. 2A and B). The apoptotic rates of the HCT116 cells treated with low, mid, and high doses of *cb*FeD were 16.6, 27.4 and 32.7%, respectively, whereas the apoptotic rate of the HCT116 cells in the control group was only 6.2%. *cb*FeD treatment produced the same effects on the SW480 cells. The results suggested that the apoptotic rate induced by *cb*FeD was increased with dose. Treatment of the cells with oxaliplatin confirmed the apoptosis of the HCT116 and SW480 cells.

Expression of p65, IκBα, p-IκBα, LC3B-I, LC3B-II and Beclin-1 in HCT116 and SW480 cells. To determine the effects of *cb*FeD on the NF-κB signaling pathway and autophagy, the expression levels of p65, IκBα, p-IκBα, LC3B-I, LC3B-II and Beclin-1 in HCT116 and SW480 cells were detected using western blot analysis (Fig. 3). In the HCT116 and SW480 cells, *cb*FeD inhibited the expression of IκBα, but enhanced the expression of p-IκBα in a dose-dependent manner. In addition, the expression of autophagic markers, including the ratio of LC3B-II and LC3B-I, and Beclin-1 were significantly decreased, suggesting *cb*FeD inhibited autophagy. The expression of p65 in the plasma was decreased, however, nuclear expression was increased, suggesting that *cb*FeD promoted the translocation of p65 into cell nuclei. Therefore, *cb*FeD may inhibit autophagy, but activate the NF-κB signaling pathway.

Effects of cbFeD on the distribution of p65 in HCT116 and SW480 cells. To further confirm the activation of the NF-κB signaling pathway by *cb*FeD, immunofluorescence staining of

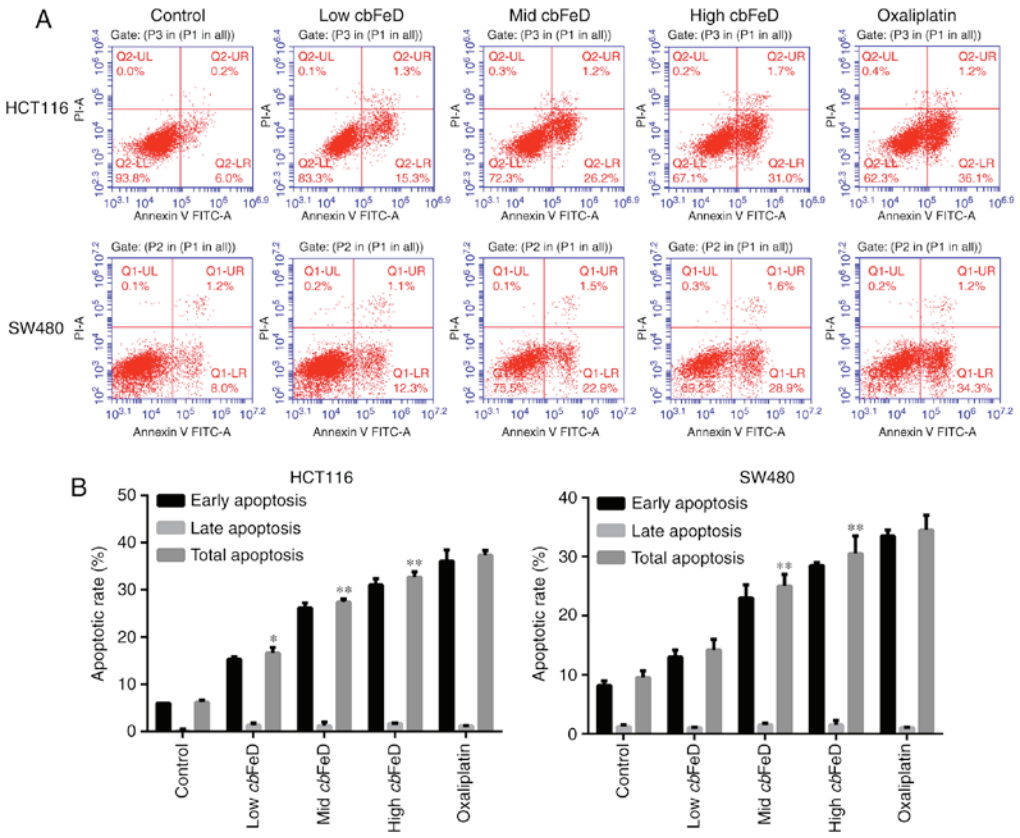

Figure 2. Effect of *cb*FeD on apoptosis of HCT116 and SW480 cells. Cells were treated with *cb*FeD-containing serum solutions prepared from mice treated by gastrogavage with saline (control), or 5 (low), 10 (mid) of 20 (high) g/kg of *cb*FeD for indicated durations. (A) Cell apoptosis was analyzed using flow cytometry and (B) apoptotic rates were calculated. Oxaliplatin was used as a control. *P<0.05 vs. control; **P<0.01 vs. control. *cb*FeD, *Codonopis bulleynana* Forest ex Diels.

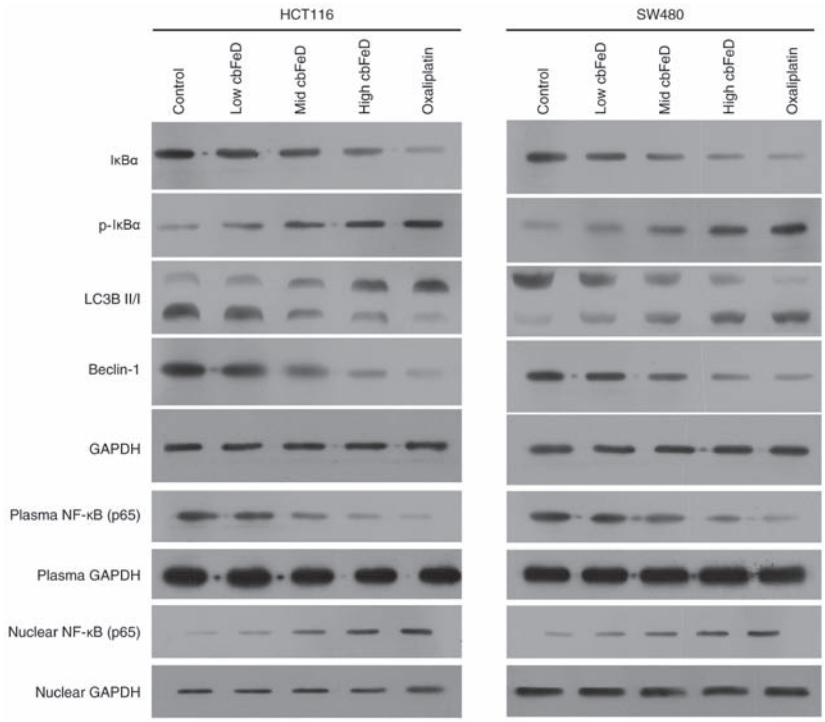

Figure 3. Effects of *cb*FeD on the expression of p65, IκBα, p-IκBα, LC3B-I, LC3B-II and Beclin-1 in HCT116 and SW480 cells. Cells were treated with *cb*FeD-containing serum solutions prepared from mice treated by gastrogavage with saline (control), or 5 (low), 10 (mid) or 20 (high) g/kg of *cb*FeD, and then the protein was extracted from cell lysate, cell plasma and cell nuclei. Expression levels of IκBα, p-IκBα, LC3B-I, LC3B-II and Beclin-1 in cell lysates of (A) HCT116 and (B) SW480 cells were detected, and expression levels of p65 in cell plasma and cell nuclei were detected using western blot analysis. Oxaliplatin was used as a control. *cb*FeD, *Codonopis bulleynana* Forest ex Diels; NF-κB, nuclear factor-κB; IκB, inhibitor of nuclear factor-κB; p-, phosphorylated; LC3, microtubule-associated protein 1 light chain 3.

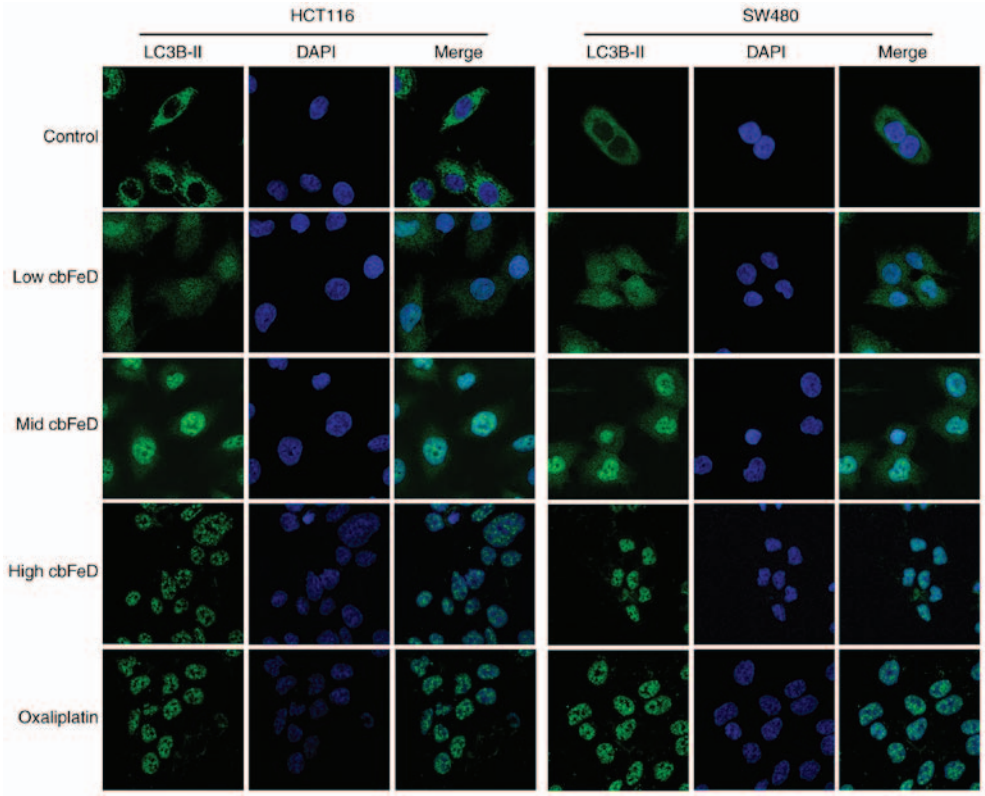

Figure 4. Immunofluorescence images of p65 in HCT116 and SW480 cells. Cells were treated with *cb*FeD-containing serum solutions prepared from mice treated by gastrogavage with saline (control), or 5 (low), 10 (mid) or 20 (high) g/kg of *cb*FeD, following by immunofluorescence staining of p65 (magnification, x200). Green, p65; blue, DAPI; Merge, p65+DAPI. *cb*FeD, *Codonopis bulleynana* Forest ex Diels.

p65 was performed. As shown in Fig. 4, p65 was present at the highest level in the cell plasma of the HCT116 and SW480 cells in the normal group. However, following treatment with a low dose of *cb*FeD, the p65 gradually entered the nuclei in the HCT116 and SW480 cells. Similar changes were observed in the mid and high dose *cb*FeD groups, with a higher dose resulting in a lower concentration of p65 in the cell plasma. This activation of the NF-κB signaling pathway was also observed following oxaliplatin treatment. Therefore, *cb*FeD activated the NF-κB signaling pathway in a dose-dependent manner.

Effects of cbFeD on the distribution of LC3B-II in HCT116 and SW480 cells. To examine the inhibition of autophagy by *cb*FeD, immunofluorescence staining of LC3B-II was performed. As shown in Fig. 5, in the normal group, high expression levels of LC3B-II were found in the HCT116 and SW480 cells. However, the expression of LC3B-II was gradually reduced with increased doses of *cb*FeD. The inhibition of autophagy by *cb*FeD was also observed in the oxaliplatin group. Therefore, *cb*FeD inhibited the autophagy of HCT116 and SW480 cells in a dose-dependent manner.

Effects of cbFeD on autophagic cells. The role of *cb*FeD in autophagy was further confirmed by AO staining and electron microscopy. As shown in Fig. 6A and B, the fluorescence intensity of AO gradually decreased with *cb*FeD treatment in a dose-dependent manner. Consistent with the AO staining, the results of the electron microscopy showed fewer autophagic vesicles in the *cb*FeD groups, compared with the number the control groups in the HCT116 and SW480 cells (Fig. 6C). Fewer autophagic vesicles were observed in cells at a higher *cb*FeD. The results of the AO staining and electron microscopy were consistent in the cells treated with oxaliplatin. Therefore, *cb*FeD inhibited autophagy in a dose-dependent manner.

PDTC inhibits the effect of cbFeD in HCT116 and SW480 cells. To investigate the effect of activation of the NF-κB signaling pathway by *cb*FeD in HCT116 and SW480 cells and its association with autophagy, PDTC was used as an inhibitor of p65 to treat the cells pretreated with *cb*FeD (Fig. 7). Following treatment with PDTC, the expression of IκBα was increased and the expression of p-IκBα was reduced (Fig. 7A). The expression of p65 in cell plasma was increased but the expression in cell nuclei was decreased, suggesting that PDTC inhibited activation of the NF-κB signaling pathway. Following inactivation of the NF-κB signaling pathway, the ratio of LC3B-II and LC3B-I, and the expression of Beclin-1 were increased. The AO staining also showed that PDTC enhanced the production of autophagic vacuole in the HCT116 and SW480 cells (Fig. 7B). The inactivation of the NF-κB signaling pathway and production of autophagic vacuoles were also observed in the oxaliplatin treatment group. Therefore, *cb*FeD inhibited autophagy via activation of the NF-κB signaling pathway.

cbFeD suppresses tumorigenicity in vivo. To confirm the above findings, particularly the results of the CCK-8 assay (Fig. 1A), and due to the fact that SW480 cells have been used in the establishment of xenograft tumors in previous studies (29,30), SW480

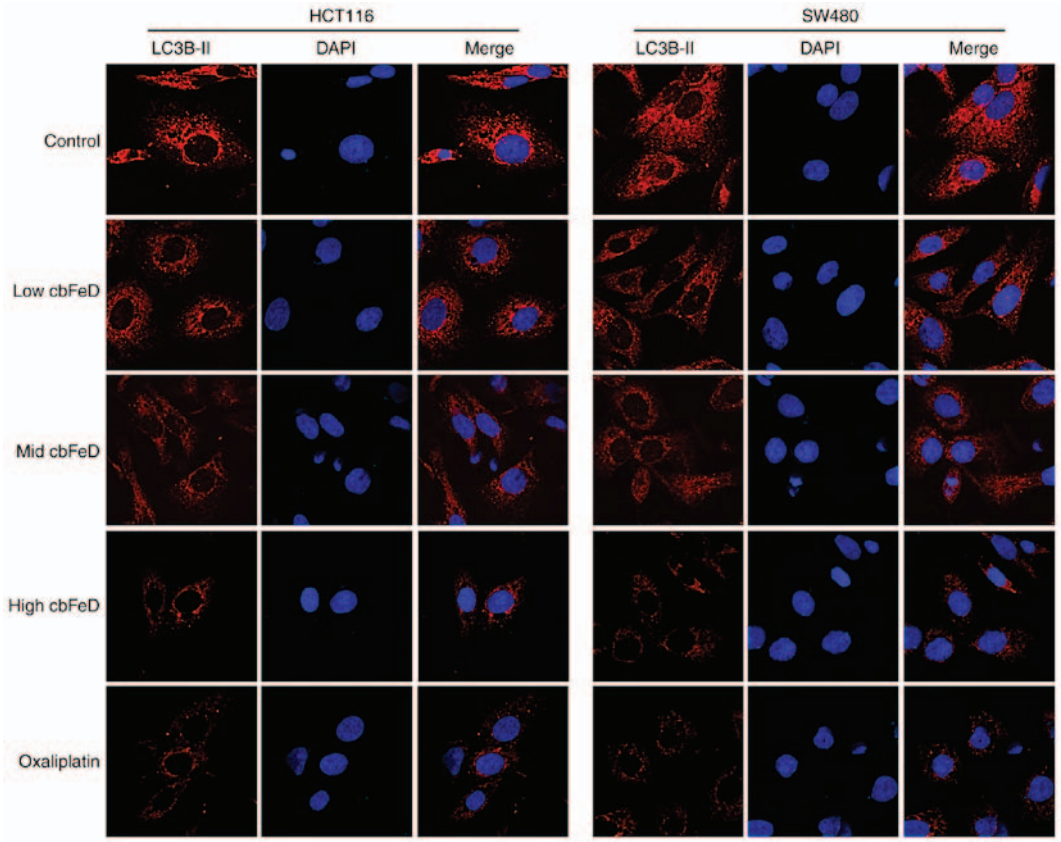

Figure 5. Immunofluorescence images of LC3B-II in HCT116 and SW480 cells. Cells were treated with *cb*FeD-containing serum solutions prepared from mice treated by gastrogavage with saline (control), or 5 (low), 10 (mid) or 20 (high) g/kg of *cb*FeD, followed by immunofluorescence staining of LC3B-II (magnification, x200). Red, LC3B-II; blue, DAPI; Merge, LC3B-II+DAPI. *cb*FeD, *Codonopis bulleyana* Forest ex Diels; LC3, LC3, microtubule-associated protein 1 light chain 3.

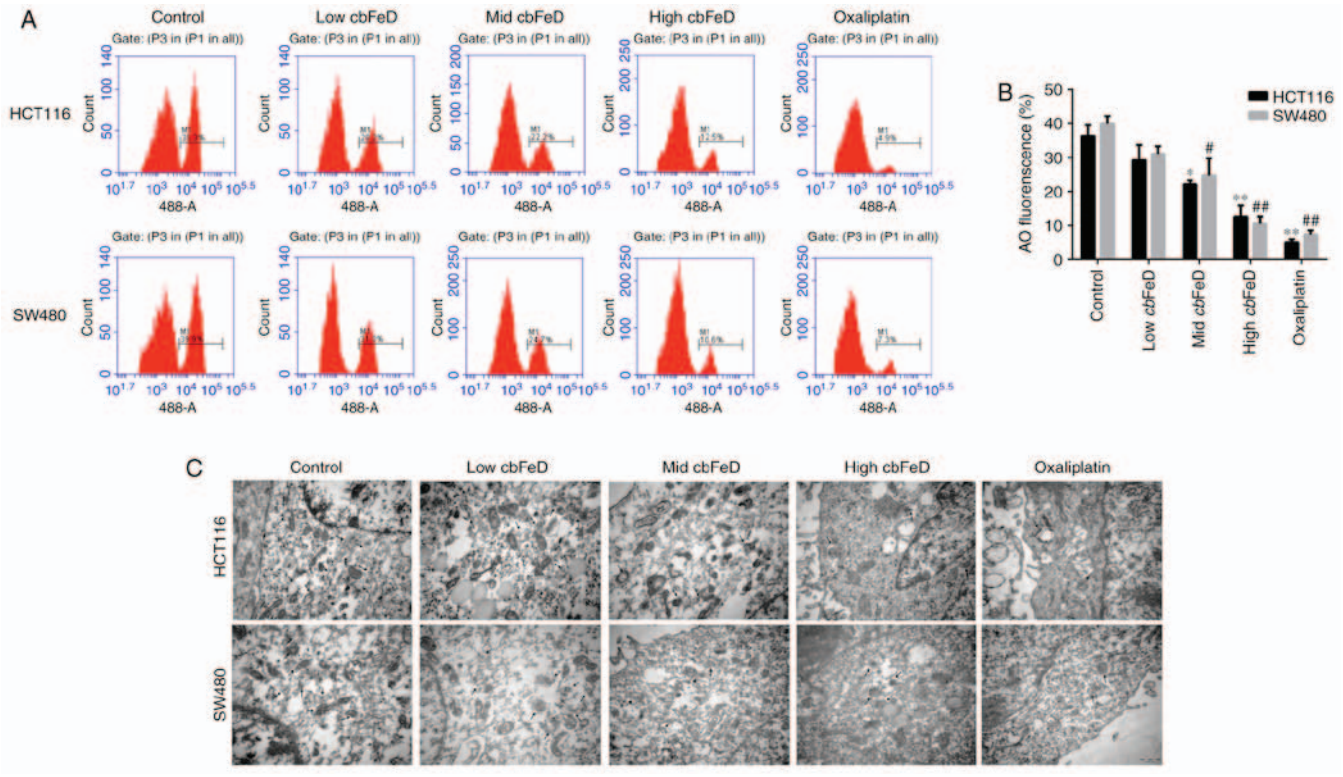

Figure 6. Detection of autophagic vacuoles by AO staining and electron microscopy. HCT116 and SW480 cells were treated with *cb*FeD-containing serum solutions prepared from mice treated by gastrogavage with saline (control), or 5 (low), 10 (mid) or 20 (high) g/kg of *cb*FeD, following which (A) AO staining and (B) quantification were performed, and (C) Electron microscopy was performed (magnification, x40,000). *P<0.05 vs. control; **P<0.01 vs. control; $^{\#}$P<0.05 vs. control; $^{\#\#}$P<0.01 vs. control. *cb*FeD, *Codonopis bulleyana* Forest ex Diels; AO, acridine orange.

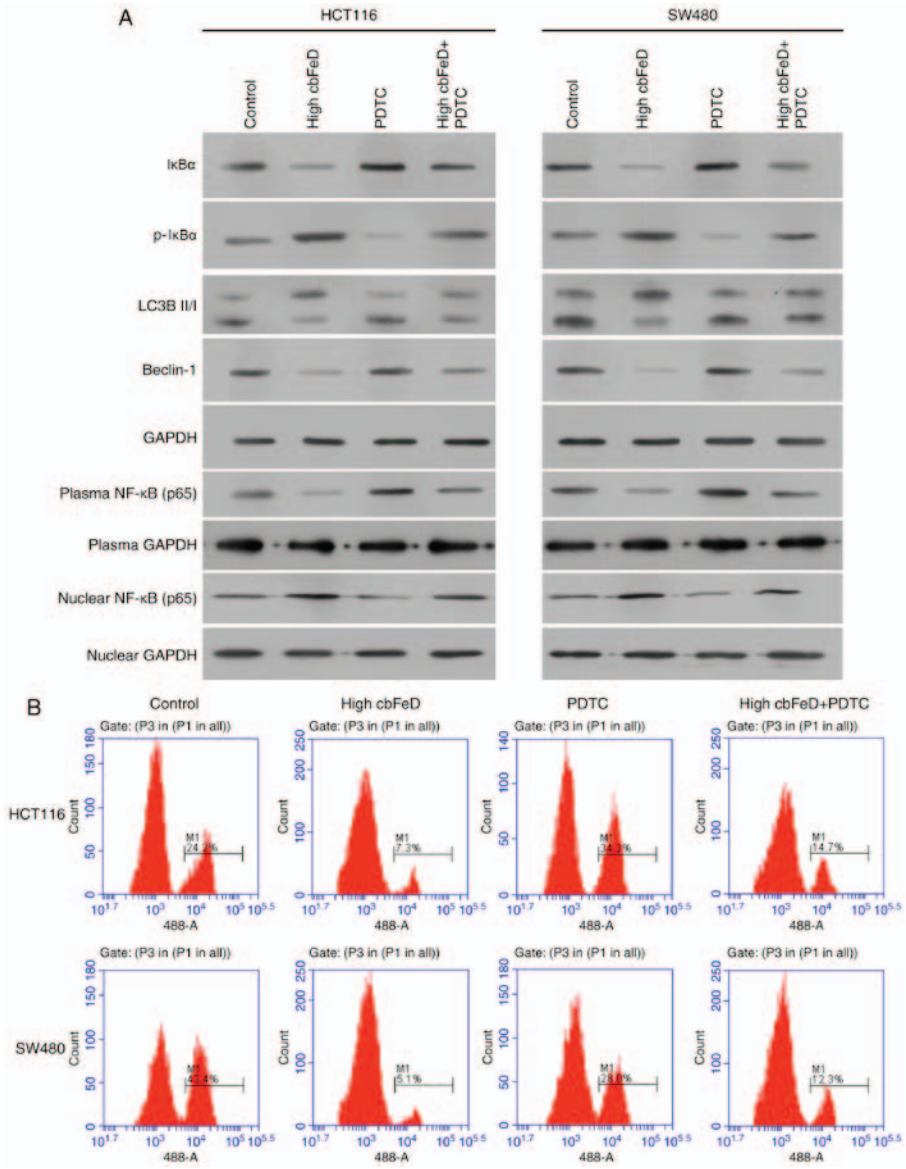

Figure 7. Effects of PDTC and a high dose of *cb*FeD on expression levels of p65, IκBα, p-IκBα, LC3B-I, LC3B-II and Beclin-1, and on autophagic vacuoles in HCT116 and SW480 cells. Cells were treated with the p65 inhibitor PDTC, with or without, *cb*FeD-containing serum solutions prepared from mice treated by gastrogavage with saline (control), or 20 (high) g/kg of *cb*FeD. (A) Expression levels of p65, IκBα, p-IκBα, LC3B-I, LC3B-II and Beclin-1 were examined using western blot analysis and (B) detection of autophagic vacuoles was performed using AO staining. *cb*FeD, *Codonopis bulleynana* Forest ex Diels; PDTC, pyrrolidine dithiocarbamate; NF-κB, nuclear factor-κB; IκB, inhibitor of NF-κB; p-, phosphorylated; LC3, microtubule-associated protein 1 light chain 3; AO, acridine orange.

cell were used to establish a nude-mouse transplanted tumor model in the present study. A high dose of *cb*FeD or oxaliplatin were administered to nude mice by gastrogavage and, 6 weeks following intragastric administration, these two groups exhibited significantly smaller tumors, compared with those in the normal saline group (Fig. 8A and B). The H&E staining showed that the *cb*FeD induced a higher level of inflammatory cell infiltration (Fig. 8C). The IHC staining of LC3B and Beclin-1 showed that the numbers of LC3B- and Beclin-1-positive cells were decreased, suggesting *cb*FeD inhibited autophagy (Fig. 8D). The results of the IHC staining of p65 showed that the number of p65-positive cells was increased, suggesting that *cb*FeD induced the activation of the NF-κB signaling pathway. The oxaliplatin control produced the same results as the tumor model. There results confirmed that *cb*FeD inhibited autophagy via activation of the NF-κB signaling pathway.

Discussion

In the present study, the antitumor effects and mechanism of *cb*FeD on human colon cancer cells were investigated *in vitro* and *in vivo* using HCT116 and SW480 colon cancer cells. The effect of oxaliplatin was also examined in colon cancer cells, which was used as a positive control.

It has been demonstrated that autophagy is involved in resistance to chemotherapy and radiotherapy (14,15). Through autophagic cells, damaged proteins or organelles are removed, which may paradoxically promote the survival of irradiated cells (18). The characteristics of the fresh root of *cb*FeD render it a unique national medicinal herb, which is used in a range of investigations in China. *cb*FeD has wide range of pharmacological effects, including anticancer effects. The anticancer role of *cb*FeD was confirmed in the present study. *cb*FeD inhibited cell

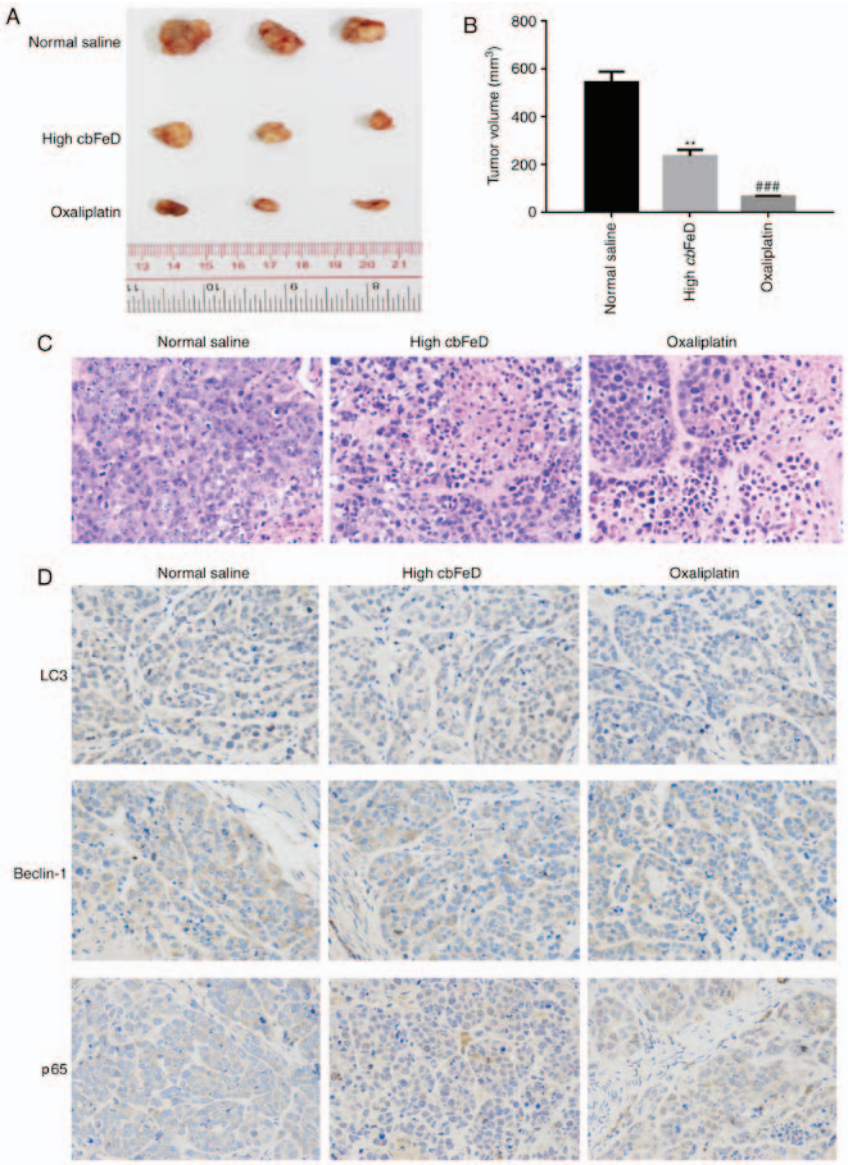

Figure 8. Effects of *cb*FeD and oxaliplatin on growth of xenograft tumors. Nude mice were subcutaneously injected in the right flank with $2.0x10^6$ SW480 cells in 0.1 ml PBS. Once tumors had formed, tumor volume was measured. The mice were then randomly divided into three groups (n=5): Normal control group, mice treated with normal saline via gavage; high *cb*FeD group, mice treated with a high dose (20 g/kg) of *cb*FeD via gavage; oxaliplatin group, mice with colon cancer treated with oxaliplatin (5 mg/kg) via gavage. After 6 weeks, the dissected tumors were collected and H&E and IHC staining were performed. (A) Tumor size. (B) tumor volume. (C) H&E staining of xenograft tumors. Magnification, x400. (D) IHC staining of p65, LC3B-II and Beclin-1. Magnification, x400. **P<0.01 and $^{###}$P<0.001 vs. control. *cb*FeD, *Codonopis bulleyana* Forest ex Diels; LC3, microtubule-associated protein 1 light chain 3; IHC, immunohistochemistry.

proliferation, increased the proportion of cells in the S phase, and promoted the apoptosis of HCT116 and SW480 cells. The inhibition of cell proliferation, and promotion of cell cycle arrest and cell apoptosis in the HCT116 and SW480 cells by *cb*FeD were found to occur in a dose-dependent manner. The inhibition of *cb*FeD in autophagy was also confirmed by various methods. Western blot analysis of the ratio of LC3B-II and LC3B-I, and the expression of Beclin-1 showed that the ratio of LC3B-II and LC3B-I and the expression of Beclin-1 were significantly decreased. The results of the AO staining showed that the numbers of autophagic cells in the HCT116 and SW480 cells were gradually reduced with increased *cb*FeD dose. Fewer autophagic vesicles were observed in the cells exposed to a higher dose of *cb*FeD, determined using electron microscopy. The inhibition of autophagy by *cb*FeD may contribute to the inhibition of cell proliferation and promotion of cell death. The results suggested that *cb*FeD is promising in sensitizing colon cancer cells to chemotherapy or radiotherapy by inducing autophagy.

It has also been suggested that *cb*FeD has a certain positive effect on chemotherapy by reducing toxicity and enhancing immune function. *cb*FeD can significantly improve the increase of hemoglobin in elderly individuals with a relatively high degree of safety (10). Previous pharmacodynamic and acute toxicity investigations of *cb*FeD have shown that it can enhance gastrointestinal peristalsis, improve tolerance to fatigue and hypoxia, and can promote the recovery of Hb, RBCs, IgG, and the immunosuppressive effect in hemorrhagic blood-deficient mice (11,12). *cb*FeD can enhance the immune function of mice with xenograft tumors, and enhance the phagocytic functions of the reticuloendothelial system (13). The NF-κB signaling pathway serves as an important regulator of immune function through the regulation of cell death and autophagy (31).

In the present study, it was found that *cb*FeD inhibited the expression of IκBα but enhanced the expression of p-IκBα. The level of p65 in plasma was decreased, however, the level in the nucleus was increased. Following treatment with a low dose of *cb*FeD, p65 entered the nuclei of HCT116 and SW480 cells. These results suggested that *cb*FeD activated the NF-κB signaling pathway. PDTC inhibits the p65-dependent activation of NF-κB (32). Following treatment of cells in the present study with PDTC, inactivation of the NF-κB signaling pathway was observed. The ratio of LC3B-II and LC3B-I, and the expression of Beclin-1 increased, the production of autophagic vacuoles in the HCT116 and SW480 cells was also increased. The role of *cb*FeD in colon cancer was further examined *in vivo* in the present study. It was found that *cb*FeD suppressed tumorigenicity *in vivo*. By treating cancer cells with *cb*FeD, cell apoptosis was increased, autophagy was inhibited and the NF-κB signaling pathway was activated. Taken together, the results of the present study showed that *cb*FeD inhibited autophagy via activation of the NF-κB signaling pathway in colon cancer cells. Therefore, *cb*FeD may be a promising Chinese herbal compound for development for use in cancer therapy.

Acknowledgements

The study was supported by the National Natural Science Foundation of China (grant no. 61363061).

References

1. Arber N and Levin B: Chemoprevention of colorectal neoplasia: The potential for personalized medicine. Gastroenterology 134: 1224-1237, 2008.
2. Yang J, Du XL, Li ST, Wang BY, Wu YY, Chen ZL, Lv M, Shen YW, Wang X, Dong DF, *et al*: Characteristics of differently located colorectal cancers support proximal and distal classification: A population-based study of 57,847 patients. PLoS One 11: e0167540, 2016.
3. Katz ML, Young GS, Zimmermann BJ, Tatum CM and Paskett ED: Assessing colorectal cancer screening barriers by two methods. J Cancer Educ: Dec 8, 2016 (Epub ahead of print).
4. Alajez NM: Large-scale analysis of gene expression data reveals a novel gene expression signature associated with colorectal cancer distant recurrence. PLoS One 11: e0167455, 2016.
5. Rocha R, Marinho R, Aparicio D, Fragoso M, Sousa M, Gomes A, Leichsenring C, Carneiro C, Geraldes V and Nunes V: Impact of bowel resection margins in node negative colon cancer. Springerplus 5: 1959, 2016.
6. Panteleimonitis S, Ahmed J, Harper M and Parvaiz A: Critical analysis of the literature investigating urogenital function preservation following robotic rectal cancer surgery. World J Gastrointest Surg 8: 744-754, 2016.
7. Sommerer C and Zeier M: Clinical manifestation and management of ADPKD in Western countries. Kidney Dis (Basel) 2: 120-127, 2016.
8. Liu D and Liang XC: New developments in the pharmacodynamics and pharmacokinetics of combination of Chinese medicine and Western medicine. Chin J Integr Med 23: 312-319, 2017.
9. Pinhua L, Yarong J, Mingyan L, Shirui L and Yaguan Z: Total flavonoids and antioxidant activity of aerial parts of *Codonopsis bulleyana*. Southwest China J Agricultural Sci 27: 1894-1898, 2014.
10. Chen Z, Li Y, Lu L, Lu B, Zhou J and HU Y: Pharmacodynamic study on Qi-Blood-Enriching effects of *Codonopis bulleynana* Fores tex Diels. Shanghai Zhong Yi Xue Yuan 43: 68-71, 2009.
11. Chen Z, Li Y, Zhou J, Wang Y, Lu B, Lu Z and Yuan J: Chou can bu tong bu wei ti qu wu dui qi xu yu xue xu dong wu mo xing de ying xiang. J Chin Med Materials 11: 1731-1733, 2009 (In Chinese).
12. Dong LD, Qian ZG, Yang Z and Cheng YX: Study on the anti-hyperlipidemia, anti-fatigue and anti-anoxia effects of *Codonopsis foetens* Hook. Yunnan Chin Med J 36: 66-68, 2015 (In Chinese).
13. Chen ZJ, Li YS, Wei QH, Chen SL and Chen DX: Effects of *Codonopis bulleynana* Forest ex Diels on enhancing sensitivity, reducing toxicity of chemotherapy and regulating immune function in Sarcoma 180 tumor-bearing mice. Chin Traditional Patent Med 34: 1848-1851, 2012 (In Chinese).
14. Whitehurst C, Pantelides ML, Moore JV, Brooman PJ and Blacklock NJ: In vivo laser light distribution in human prostatic carcinoma. J Urol 151: 1411-1415, 1994.
15. Xiong L, Liu Z, Ouyang G, Lin L, Huang H, Kang H, Chen W, Miao X and Wen Y: Autophagy inhibition enhances photocytotoxicity of Photosan-II in human colorectal cancer cells. Oncotarget 8: 6419-6432, 2017.
16. Shintani T and Klionsky DJ: Autophagy in health and disease: A double-edged sword. Science 306: 990-995, 2004.
17. Rubinsztein DC, Gestwicki JE, Murphy LO and Klionsky DJ: Potential therapeutic applications of autophagy. Nat Rev Drug Discov 6: 304-312, 2007.
18. Panganiban RA, Snow AL and Day RM: Mechanisms of radiation toxicity in transformed and non-transformed cells. Int J Mol Sci 14: 15931-15958, 2013.
19. Chen ST, Lee TY, Tsai TH, Lin YC, Lin CP, Shieh HR, Hsu ML, Chi CW, Lee MC, Chang HH and Chen YJ: The Traditional Chinese Medicine DangguiBuxue tang sensitizes colorectal cancer cells to chemoradiotherapy. Molecules 21: pii:E1677, 2016.
20. Wang M, Tan W, Zhou J, Leow J, Go M, Lee HS and Casey PJ: A small molecule inhibitor of isoprenylcysteine carboxymethyltransferase induces autophagic cell death in PC3 prostate cancer cells. J Biol Chem 283: 18678-18684, 2008.
21. Wang B, Qiao L, Shi Y, Feng X, Chen D and Guo H: ASPP2 inhibits oxaliplatin-induced autophagy and promotes apoptosis of colon cancer cells. Xi Bao Yu Fen Zi Mian Yi Xue Za Zhi 31: 898-904, 2015 (In Chinese).
22. Tan S, Peng X, Peng W, Zhao Y and Wei Y: Enhancement of oxaliplatin-induced cell apoptosis and tumor suppression by 3-methyladenine in colon cancer. Oncol Lett 9: 2056-2062, 2015.
23. O'Donovan TR, Rajendran S, O'Reilly S, O'Sullivan GC and McKenna SL: Lithium modulates autophagy in esophageal and colorectal cancer cells and enhances the efficacy of therapeutic agents in vitro and in vivo. PLoS One 10: e0134676, 2015.
24. Shan J, Xuan Y, Zhang Q, Zhu C, Liu Z and Zhang S: Ursolic acid synergistically enhances the therapeutic effects of oxaliplatin in colorectal cancer. Protein Cell 7: 571-585, 2016.
25. Lu YX, Ju HQ, Wang F, Chen LZ, Wu QN, Sheng H, Mo HY, Pan ZZ, Xie D, Kang TB, *et al*: Inhibition of the NF-κB pathway by nafamostat mesilate suppresses colorectal cancer growth and metastasis. Cancer Lett 380: 87-97, 2016.
26. Zeng Y, Liu XH, Tarbell J and Fu B: Sphingosine 1-phosphate induced synthesis of glycocalyx on endothelial cells. Exp Cell Res 339: 90-95, 2015.
27. Paglin S, Hollister T, Delohery T, Hackett N, McMahill M, Sphicas E, Domingo D and Yahalom J: A novel response of cancer cells to radiation involves autophagy and formation of acidic vesicles. Cancer Res 61: 439-444, 2001.
28. Dutta D, Chakraborty B, Sarkar A, Chowdhury C and Das P: A potent betulinic acid analogue ascertains an antagonistic mechanism between autophagy and proteasomal degradation pathway in HT-29 cells. BMC Cancer 16: 23, 2016.
29. Chen SL, Cai SR, Zhang XH, Li WF, Zhai ET, Peng JJ, Wu H, Chen CQ, Ma JP, Wang Z and He YL: Targeting CRMP-4 by lentivirus-mediated RNA interference inhibits SW480 cell proliferation and colorectal cancer growth. Exp Ther Med 12: 2003-2008, 2016.
30. Jiang H, Ju H, Zhang L, Lu H and Jie K: microRNA-577 suppresses tumor growth and enhances chemosensitivity in colorectal cancer. J Biochem Mol Toxicol: Feb 2, 2017 (Epub ahead of print). doi: 10.1002/jbt.21888.
31. Baldwin AS: Regulation of cell death and autophagy by IKK and NF-kappaB: Critical mechanisms in immune function and cancer. Immunol Rev 246: 327-345, 2012.
32. Samuel T, Fadlalla K, Gales DN, Putcha BD and Manne U: Variable NF-κB pathway responses in colon cancer cells treated with chemotherapeutic drugs. BMC Cancer 14: 599, 2014.